

# Lung ultrasound: an opportunity to increase the accuracy of the physical examination by the nephrologist

Marcus Gomes Bastos<sup>1\*</sup> 

## INTRODUCTION

Point-of-care ultrasound (POCUS) performed at the bedside by the attending physician is primarily meant to provide answers to focused questions to narrow the differential diagnosis and guide clinical therapy practically in all medical specialties, ranging from the emergency department to ambulatory clinics<sup>1,2</sup>. One of the main applications of POCUS is lung ultrasound (LUS). Initially used by intensive care and emergency physicians, LUS was soon embraced by cardiologists. However, among Brazilian nephrologists who already use POCUS, only 31% use LUS routinely<sup>3</sup>.

The main indications of LUS are for the diagnosis of pneumothorax, acute pulmonary edema, pleural effusion, infectious pathologies (bacterial and viral pneumonia), acute respiratory distress syndrome, asthma, and chronic obstructive pulmonary disease. In contrast, the main limitations of using LUS are subcutaneous emphysema (the sound wave cannot pass through subcutaneous air), large pneumothorax, large surgical dressings, and body fat in morbidly obese individuals<sup>4,5</sup>. With the recent disponibility at low cost and highly portable handheld ultrasound, the most important barrier to implementing LUS into routine clinical practice is still the scarcity of well-trained faculty able to conduct training and apply LUS at the bedside.

In this minireview article, we discussed some technical aspects of LUS and how the lung artifacts generated can be used by nephrologists to diagnose pneumothorax, pleural effusion, and pulmonary congestion in patients with renal diseases.

## TECHNICAL ASPECTS OF LUS

Lichtenstein et al.<sup>4</sup> was the first to demonstrate that interpretation of artifacts makes it possible to diagnose pleuro-pulmonary

pathologies with LUS. However, it is necessary to warn that LUS is not anatomical; it only identifies pathologies that “touch” the pleura and that the lung parenchyma, when viewed at LUS, is always pathological. In contrast, we can infer that the lung is normal if we observe lung sliding, A-Lines, and the curtain sign at the lung bases<sup>5</sup>.

Figure 1 (left and right) shows the structures that make up the chest wall anatomically and their corresponding US images. The top of the US viewing screen is always where the transducer touches the patient’s skin. The transducer should be held like a pen, with its orientation marker pointing toward the head. When using lung or abdominal exam presetting, the screen marker will appear on the viewing screen’s upper left side. As the transducer’s orientation marker and the viewing screen marker point in the same direction, the screen’s left side will be cephalad and the right side will be caudad. Comparing both figures and looking from top to bottom, we identify the skin and subcutaneous tissue, then the pectoral and intercostal muscles, the ribs (with posterior acoustic shadow), and the pleural line (parietal and visceral pleura). Below the pleural line and between the ribs, anatomically is the lung, but in the

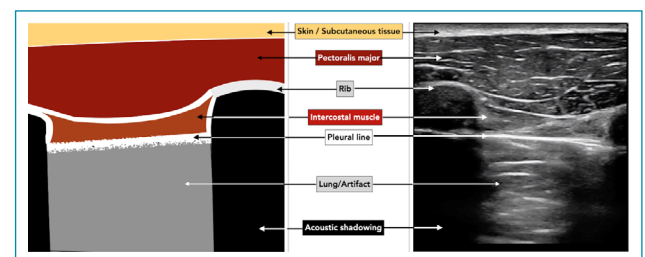


**Figure 1.** Drawing (left) and ultrasound image (right) showing the structures that make up the chest wall.

<sup>1</sup>Universidade Federal de Juiz de Fora, Faculdade de Medicina, Programa de Pós-Graduação em Saúde – Juiz de Fora (MG), Brazil.

\*Corresponding author: [marcusbastos7@gmail.com](mailto:marcusbastos7@gmail.com)

Conflicts of interest: the authors declare there is no conflicts of interest. Funding: this study received financial support from Fundação IMEPEN. Received on August 20, 2021. Accepted on September 04, 2021.

LUS, the corresponding images are artifacts produced by the sound waves' scattering.

To obtain the images in the LUS, we can use high- and low-frequency transducers (or probes). However, depending on the pathology assessed, we might select a determined transducer. For instance, if the suspicion is pneumothorax, a high-frequency transducer (with higher image resolution) allows a more detailed analysis of the pleura line. In contrast, the convex and phased-array probes (longer wavelengths that penetrate deep structures) are most often used to identify pleural effusion and pulmonary congestion<sup>5,6</sup>.

Understanding the equipment controls is essential to optimize and interpret the images obtained with the LUS. The most significant adjustments are:

1. Gain control increases brightness by increasing the amplitude of returning US waves;
2. Time gain compensation controls are intended to compensate for the attenuation of sound waves that occur with depth;
3. Depth control alters the scanning depth displayed on the screen; and
4. The focal point indicates where maximum resolution occurs. In contrast, tissue harmonic imaging, a tool for improving contrast resolution and lateral resolution, and the multi-beam, features that enhance the image's quality should be disabled to facilitate the recognition of the pulmonary artifacts, of paramount importance in LUS<sup>5</sup>.

In practical terms, a simple, accurate, and efficient lung exam protocol divides the chest into three zones per hemithorax:

1. Anterior, superior, and inferior;
2. Lateral, superior, and inferior; and
3. Posterior, superior, and inferior.

The choice of a specific region in the evaluation with LUS depends on the pretest probability. For instance, if the diagnostic suspicion is pneumothorax, the scanning should begin in the upper anterior region in a patient in the supine position. In contrast, if the diagnostic suspicion is pleural effusion, the examination should start in the lower lateral region<sup>6</sup>.

## LUNG ARTIFACTS

As mentioned, LUS is based on the interpretation of artifacts<sup>4,6</sup>; the main ones are:

1. Lung or pleural sliding;
2. A-lines;
3. B-lines;
4. The mirror image of the liver or spleen;
5. The thoracic spine sign; and
6. The curtain sign<sup>5,6</sup>.

To obtain an adequate acoustic window for LUS, the transducer should be positioned as perpendicular as possible to the pleura and the images are obtained in the sagittal, oblique, or parallel to two ribs<sup>7</sup>.

The lung or pleural sliding artifact is a normal finding and appears as a shimmering or sliding of the visceral pleura against the parietal pleura during the respiratory cycle. It is identified as a hyperechoic (white) line located a few millimeters below the ribs and can be evaluated using linear, convex, and phased-array transducers (Figure 1). A health pleura should be uniformly thin (<0.3 mm) without irregularities<sup>5,7</sup>.

In case of difficulty to confirm lung sliding by B-mode, an alternative is to use the M-mode, which depicts the tissues' movement along a single scan line over time. The chest wall is less mobile in normal conditions, appearing as a series of horizontal lines, whereas the lung parenchyma is more mobile; it moves back and forth, giving it a grainy appearance by M-mode.

The A-lines are artifacts that originate from the reverberation of sound waves between two highly reflective surfaces, i.e., the US transducer and the pleural line<sup>5,6</sup>. They appear as horizontal lines deep to the pleural line. A-lines are identified as repetitive hyperechoic horizontal lines equidistant from the pleural line and each other (Figure 2A). The A-lines mean air-filled lungs<sup>5-7</sup>.

The B-lines have a complex and incompletely understood pathophysiology. The normal interlobular and intralobular septa are below the resolution of standard US frequencies, and US waves cannot propagate in air-filled lungs. As soon as the septa are widened or distended with interstitial fluid, fibrous tissue, collagen, or cellular deposition, US waves can propagate into the lung and are seen as B-lines<sup>7</sup>. The B-lines are vertical hyperechoic lines, which emanate from the pleural line, move with the breathing cycle, erase the A-lines, and extend to the viewing screen's lower limit (Figure 2B). The finding of three or more B-lines between two ribs indicates interstitial pulmonary syndrome, such as pulmonary congestion<sup>8,9</sup>.

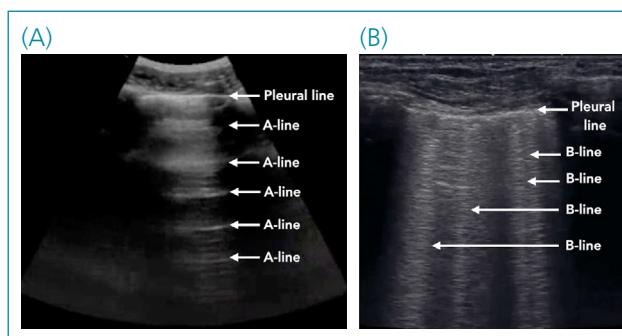


**Figure 2.** (A) Lung ultrasound showing the pleural line and the artifact A-line and (B) Lung ultrasound displaying the artifact B-line.

The comet tail is a short reverberation artifact, hyperechoic, move with lung sliding, whose appearance is obviously different from B-lines and can be seen in normal lungs<sup>10,11</sup>.

The mirror image artifact of the liver or spleen corresponds to these organs' supposed presence above the diaphragm. US images originate from the intensity and the time when the sound beams take back to the transducer. When the sound waves encounter a highly reflective structure like the diaphragm, the sound beams suffer multiple reflections on the way back to the transducer<sup>5</sup>. However, the US machine's processor interprets that the sound waves were obtained along a straight line. Two images, i.e., the actual image below the diaphragm (liver or spleen) and the mirror image above, are generated, resulting in a mirror artifact. In Figure 3, the image obtained in the upper right quadrant region, at the middle axillary line, one

can identify the liver, the diaphragm, and, above them, the mirror image of the liver<sup>7</sup>.

The vertebral bodies correspond to a wavy hyperechoic (white) line posterior to the liver (or spleen) and the kidney (Figure 3). Under normal conditions, the vertebral bodies are visualized only up to the diaphragm limit. Above the diaphragm, the air-filled lungs block the passage of sound, preventing vertebral bodies' visualization<sup>5,7,12</sup>. The thoracic spine sign is the spine's visualization above the diaphragm level, most commonly due to pleural effusion; however, it can also occur with hemothorax and lung consolidation.

The curtain sign is seen in healthy and aerated lungs. An air-filled lung is like a "curtain" that sweeps down and over the other organs, momentarily obscuring them during the respiratory cycle. Thus, the diaphragm, liver, or spleen disappears during inspiration and reappears during expiration.

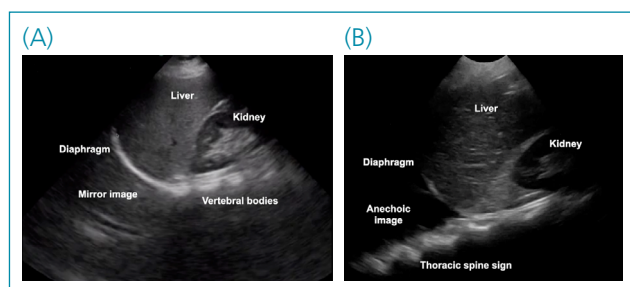


**Figure 3.** The ultrasound image obtained in the right upper quadrant. (A) Normal findings and (B) Pleural effusion is characterized by an anechoic image above the diaphragm and thoracic spine sign.

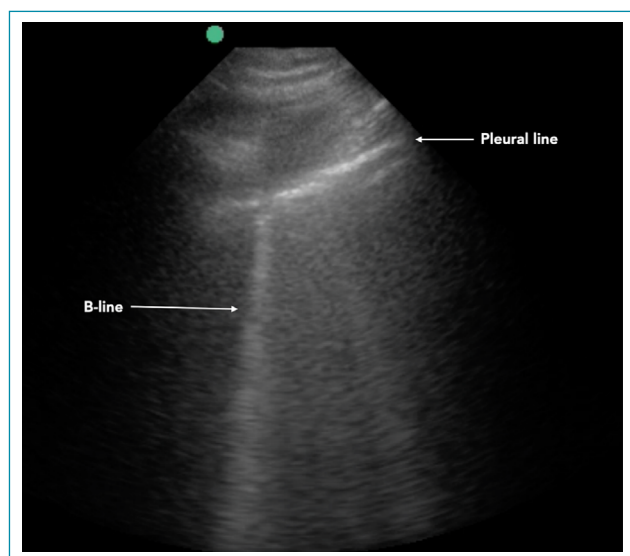


**Figure 4.** Lung ultrasound from a patient with COVID-19 showing an irregular and fragmented pleural line from which a B-line originates.

## MOST IMPORTANT CLINICAL USE OF LUNG ULTRASOUND IN NEPHROLOGY

### Diagnosis of pneumothorax

Central venous access is a routine procedure in nephrology but often proves to be challenging. Although US was first used to facilitate vascular access almost 40 years ago<sup>13</sup>, most Brazilian nephrologists still perform the procedure based on anatomical landmarks<sup>3</sup>. This procedure would be much easier and safer if guided by ultrasonography, which allows the visualization of the internal jugular vein, the carotid artery, and the needle in the same path, thus minimizing the possibility of puncture accidents. Cannulation of the internal jugular vein with real-time US guidance is now standard practice and is highly recommended by many societies and supported by evidence<sup>12-16</sup>. Thus, US-guided central venous access makes the procedure safer for the patient and the nephrologist.

The pneumothorax assessment is usually done in the patient in the supine position and scanning the anterior and upper chest wall. The three transducers commonly used to obtain images in internal medicine can be used. The high-frequency linear probe with a frequency between 5 and 13 MHz offers excellent image resolution but a maximum useful imaging depth of approximately 6 cm. Convex probe (frequency between 2 and 5 MHz) and phased-array probe (frequency between 1 and 5 MHz) provide a deeper penetration to depths around 22 cm but at the expense of lower resolution. Several different sonographic signs can be used to rule in or rule out pneumothorax, specifically, lung sliding, B-lines, lung point, and the findings on M-Mode<sup>5-7</sup>.

As previously mentioned, when the visceral and parietal pleura are opposed and normal respiration occurs, a shimmering of the visceral on parietal pleura will be observed, essentially ruling out any air between both pleurae with nearly 100% sensitivity<sup>17,18</sup>. The other indications that the visceral and parietal pleura are in touch is observing the artifact B-lines, which emanate from the pleural line. The visualization of the lung sliding and/or the B-lines rules out pneumothorax diagnosis in the examined area in most circumstances. However, when air interposes between the two pleurae, as in the pneumothorax, it is only possible to see the parietal pleura; therefore, the lung sliding and/or B-lines are no more seen. The absence of lung sliding may indicate pneumothorax in an appropriate clinical context but is also seen in other clinical conditions, such as shallow and rapid breathing, apnea, pneumonia, atelectasis, pleural adhesions, previous pleurodesis, and selective orotracheal intubation.

Alternatively, pneumothorax can be assessed using the M-mode<sup>6,7</sup>. Typically, the near field, which is superficial to the pleural line, is not moving and appears in straight parallel lines. The far-field, deep to the pleural line, is shimmering back and forth and appears grainy, known as the seashore sign. In contrast, when air interposes between the visceral and parietal pleurae, the last structure seen is the visceral pleura, which will appear as a fixed, white, hyperechoic line. Thus, the chest wall still appears as straight parallel lines on M-mode, but since no lung sliding is visualized, the area deep to the pleural line also appears as straight parallel lines; this is known as the barcode sign.

However, the findings at LUS that rule in the diagnosis of pneumothorax is the lung point sign<sup>5,7,19</sup>. The lung point marks the location on the chest wall where the collapsed lung meets the parietal pleura, seen as inspiratory presence and expiratory absence of lung sliding in a determined point of examination. On M-mode, seashore and barcode signs are seen, which vary with the respiratory cycle. The lung point identification is made by moving the transducer around the chest wall, from areas of lung sliding to areas without lung sliding, until both are seen in the same location. The lung point sign is highly specific<sup>20</sup> but presents relatively low sensitivity in the diagnosis of pneumothorax<sup>21</sup>.

In a systematic review and meta-analysis (1,048 participants) to compare the diagnostic accuracy of US with that of chest radiography in patients with suspected pneumothorax secondary to trauma (767 participants) and iatrogeny (281 participants), it was found that pooled estimates of sensitivity were 90.9% (95%CI 86.5–93.9%) for the LUS and 50.2% (95%CI 43.5–57.0%) for chest radiography. Pooled estimates of specificity were 98.2% (95%CI 97.0–99.0%) for LUS and 99.4% (95%CI 98.3–99.8%) for chest radiography<sup>21,22</sup>.

## Diagnosis of pleural effusion

Another use of LUS is in diagnosing pleural effusion<sup>5-7,20</sup>. Pleural effusion may be classified into a transudate or an exudate. The majority of the pleural effusion seen in renal patients is transudate secondary to conditions that cause an increase in the pulmonary capillary hydrostatic pressure or a decrease in the oncotic capillary pressure (e.g., nephrotic syndrome and end-stage renal disease)<sup>23,24</sup>. Less frequently, pleural effusion can be due to the retroperitoneal leakage of urine via the diaphragmatic lymphatics (urinothorax)<sup>25</sup> or originate from the movement of dialysate from the peritoneal to the pleural cavity across the diaphragm in a patient undergoing peritoneal dialysis<sup>26</sup>.

Pleural fluid accumulates in the posterolateral costophrenic recesses, the most dependent portions of the thorax in upright patients. Thus, in ambulatory patients, the US examination is usually performed with the patient in an upright position. In contrast, in hospitalized or critically ill patients, the examination is in a supine or semi-recumbent position. The transducers used are of low frequency and longer wavelengths (convex or phased-array) that penetrate deep structures. The transducer is positioned on the chest with the marker point cephalad; consequently, the patient's head is always toward the left of the viewing screen.

The three most critical sonographic findings in pleural effusion diagnosis are the presence of the thoracic spine sign, the absence of the mirror artifact, and the absence of the curtain sign<sup>5,7</sup>. Unlike a normal air-filled lung that blocks any sound waves from passing, in pleural effusions, sound waves can pass through the pleural fluid, allowing the spine's visualization also above the diaphragm (the thoracic spine sign). Additionally, the mirror artifact is substituted by an anechoic image of fluid-filled material above the diaphragm (Figure 3). Finally, the fluid-filled pleura does not allow the aerated lung to descend into the scanning field at the diaphragm level during inspiration, precluding the visualization of the curtain sign<sup>5,7,27</sup>.

In a systematic review with meta-analysis on the accuracy of sonography for detecting pleural effusion using computed tomography or thoracic drainage as a reference, LUS showed consistently high average sensitivity (93%), specificity (96%), and accuracy for detecting pleural effusion<sup>28</sup>. Besides, it allows the identification of pleural effusion as less as 20 mL<sup>29</sup>.

## Diagnosis of pulmonary congestion

LUS is a simple, noninvasive, and semiquantitative tool to assess interstitial lung syndrome. B-lines are a surrogate for the alveolar–interstitial syndrome, with pulmonary congestion being the most frequent pulmonary complication found in patients with kidney disease<sup>5-7</sup>. Volume overload in hemodialysis patients is an independent risk factor for death from

cardiovascular events<sup>30</sup>. Notably, the number of B-lines has an excellent correlation with the severity of fluid accumulation in the lung. In hypervolemic patients who present a low glomerular filtration rate, the number of B-lines increases as pulmonary extravascular water accumulates<sup>31</sup>. Eventually, they converge into vertical sheets (white lung) seen in both lungs. Another interesting finding is that B-lines are highly dynamic, decreasing in number with fluid removal during a hemodialysis session<sup>32</sup>. They are also more sensitive than auscultation of pulmonary crackles in the diagnosis of asymptomatic pulmonary congestion, in addition to being a strong and independent predictor for fatal and nonfatal cardiac events and mortality from all causes<sup>33</sup>.

The scanning technique uses a low-frequency convex or phased-array transducer to scan the thoracic cavity to get a good sense of interstitial lung syndrome distribution<sup>6,7</sup>.

Various protocols have been used to assess lung congestion by B-lines. A 28-zone protocol for both hemithorax is used mainly for research purposes<sup>32,33</sup>. A more practical approach is the four-zone per hemithorax scanning method in the semi-quantitative evaluation of interstitial lung syndrome. However, for diagnosis, a two-zone protocol is sufficient. The presence of interstitial syndrome due to extravascular lung water is defined as three or more B-lines between two rib spaces seen in two or more positive interspaces bilaterally<sup>5,7</sup>. This approach presents a high sensitivity of 85.7% and specificity of 97.7% for alveolar-interstitial syndrome compared with chest radiography<sup>6,34,35</sup>.

B-lines show high sensitivity as a manifestation of pulmonary congestion but low specificity; they are also seen in other

interstitial lung syndromes, such as pulmonary fibrosis, infection (pneumonia and COVID-19), atelectasis, pulmonary contusion, pulmonary infarction, or neoplasia<sup>5-7,36</sup>. At present, in the context of the COVID-19 pandemic, B-lines characteristics may help distinguish COVID-19 pneumonia from pulmonary congestion in dyspneic patients. In COVID-19, the B-lines originate from a pleural line often irregular, fragmented, and are patchy, non-gravity related in distribution, more often coalescent, and with defined spared lung areas (Figure 4). In contrast, in cardiogenic pulmonary edema, the B-lines originate from a pleural line usually thin, regular, and homogeneous and are gravity-related distributed bilaterally, more frequently separated or coalescent in more severe cases, and with no pulmonary spared areas (Figure 2B)<sup>36</sup>.

## CONCLUSIONS

LUS allows the nephrologist to evaluate pulmonary pathologies that can occur in different nephrological scenarios and reduce other imaging methods (X-ray and computed tomography) that use ionizing radiation. The portability, broad availability, and improved technology of US devices and their practical utility as diagnostic, monitoring, and procedural guidance tools allow to carry out LUS in different practice environments such as nephrological offices, dialysis rooms, and intensive care units. Proficiency in LUS increases the physical examination accuracy in diagnosing pneumothorax, pleural effusion, and pulmonary congestion at the bedside and enables better nephrological practice.

## REFERENCES

- Kendall JL, Hoffenberg SR, Smith RS. History of emergency and critical care ultrasound: the evolution of a new imaging paradigm. *Crit Care Med*. 2007;35(5 Suppl):S126-30. <https://doi.org/10.1097/01.CCM.0000260623.38982.83>
- Moore CL, Copel JA. Point-of-care ultrasonography. *N Engl J Med*. 2011;364(8):749-57. <https://doi.org/10.1056/NEJMra0909487>
- Bastos MG, Vieira AL, Nascimento MM, Barros E, Pazeli Jr JM, Kirsztajn GM. Ultrasonografia point-of-care em nefrologia: uma pesquisa nacional transversal entre nefrologistas brasileiros. *J Bras Nefrol*. 2021;43(1):68-73. <https://doi.org/10.1590/2175-8239-JBN-2020-0023>
- Lichtenstein D, Mézière G, Biderman P, Gepner A, Barré O. The comet-tail artifact. An ultrasound sign of alveolar-interstitial syndrome. *Am J Respir Crit Care Med*. 1997;156(5):1640-6. <https://doi.org/10.1164/ajrccm.156.5.96-07096>
- Lichtenstein DA. Introduction to lung ultrasound. In: Lichtenstein DA, editor. *Whole body ultrasonography in the critically ill*. Berlin: Springer-Verlag; 2010. p. 117-27.
- Volpicelli G, Elbarbary M, Blaivas M, Lichtenstein DA, Mathis G, Kirkpatrick AW, et al. International evidence-based recommendations for point-of-care lung ultrasound. *Intensive Care Med*. 2012;38(4):577-91. <https://doi.org/10.1007/s00134-012-2513-4>
- Soni N, Arntfield R, Kory P. *Point-of-care ultrasound*. 2nd ed. Philadelphia: Elsevier; 2019.
- Picano E, Pellikka PA. Ultrasound of extravascular lung water: a new standard for pulmonary congestion. *Eur Heart J*. 2016;37(27):2097-104. <https://doi.org/10.1093/eurheartj/ehw164>
- Petrzellini MF, Vasti MP, Errico A, D'Agostino R, Tramacere F, Gianicolo EAL, et al. Ultrasound B-lines for detection of late lung fibrosis in breast cancer patients after radiation therapy. *Ann Ist Super Sanita*. 2018;54(4):294-9. [https://doi.org/10.4415/ANN\\_18\\_04\\_05](https://doi.org/10.4415/ANN_18_04_05)
- Lichtenstein D, Mézière G, Biderman P, Gepner A, Barré O. The comet-tail artifact. An ultrasound sign of alveolar-interstitial syndrome. *Am J Respir Crit Care Med*. 1997;156(5):1640-6. <https://doi.org/10.1164/ajrccm.156.5.96-07096>

11. Lee FCY, Jenssen C, Dietrich CF. A common misunderstanding in lung ultrasound: the comet tail artefact. *Med Ultrason*. 2018;20(3):379-84. <https://doi.org/10.11152/mu-1573>
12. Soni NJ, Franco R, Velez MI, Schnobrich D, Dancel R, Restrepo MI, et al. Ultrasound in the diagnosis and management of pleural effusions. *J Hosp Med*. 2015;10(12):811-6. <https://doi.org/10.1002/jhm.2434>
13. Olsen TCR, Rimstad IJ, Tarpgaard M, Holmberg S, Hallas P. Current use of ultrasound for central vascular access in children and infants in the Nordic countries: a cross-sectional study. *J Vasc Access*. 2015;16(2):148-51. <https://doi.org/10.5301/jva.5000326>
14. Troianos CA, Hartman GS, Glas KE, Skubas NJ, Eberhardt RT, Walker JD, et al. Special articles: guidelines for performing ultrasound guided vascular cannulation: recommendations of the American Society of Echocardiography and the Society of Cardiovascular Anesthesiologists. *Anesth Analg*. 2012;114(1):46-72. <https://doi.org/10.1213/ANE.0b013e3182407cd8>
15. Lamperti M, Bodenham AR, Pittiruti M, Blaivas M, Augoustides JG, Elbarbary M, et al. International evidence-based recommendations on ultrasound-guided vascular access. *Intensive Care Med*. 2012;38(7):1105-17. <https://doi.org/10.1007/s00134-012-2597-x>
16. AIUM practice guideline for the use of ultrasound to guide vascular access procedures. *J Ultrasound Med*. 2013;32(1):191-215. <https://doi.org/10.7863/jum.2013.32.1.191>
17. Rowan KR, Kirkpatrick AW, Liu D, Forkheim KE, Mayo JR, Nicolaou S. Traumatic pneumothorax detection with thoracic US: correlation with chest radiography and CT-initial experience. *Radiology*. 2002;225(1):210-4. <https://doi.org/10.1148/radiol.2251011102>
18. Blaivas M, Lyon M, Duggal S. A prospective comparison of supine chest radiography and bedside ultrasound for the diagnosis of traumatic pneumothorax. *Acad Emerg Med*. 2005;12(9):844-9. <https://doi.org/10.1197/j.aem.2005.05.005>
19. Mayo PH, Copetti R, Feller-Kopman D, Mathis G, Maury E, Mongodi S, et al. Thoracic ultrasonography: a narrative review. *Intensive Care Med*. 2019;45(9):1200-11. <https://doi.org/10.1007/s00134-019-05725-8>
20. Chan SSW. Emergency bedside ultrasound to detect pneumothorax. *Acad Emerg Med*. 2003;10(1):91-4. <https://doi.org/10.1111/j.1553-2712.2003.tb01984.x>
21. Alrajhi K, Woo MY, Vaillancourt C. Test characteristics of ultrasonography for the detection of pneumothorax: a systematic review and meta-analysis. *Chest*. 2012;141(3):703-8. <https://doi.org/10.1378/chest.11-0131>
22. Lichtenstein D, Mezière G, Biderman P, Gepner A. The "lung point": an ultrasound sign specific to pneumothorax. *Intensive Care Med*. 2000;26(10):1434-40. <https://doi.org/10.1007/s001340000627>
23. Storto ML, Kee ST, Golden JA, Webb WR. Hydrostatic pulmonary edema: high-resolution CT findings. *AJR Am J Roentgenol*. 1995;165(4):817-20. <https://doi.org/10.2214/ajr.165.4.7676973>
24. Hull RP, Goldsmith DJA. Nephrotic syndrome in adults. *BMJ*. 2008;336(7654):1185-9. <https://doi.org/10.1136/bmj.39576.709711.80>
25. Baron RL, Stark DD, McClennan BL, Shanes JG, Davis GL, Koch DD. Intrathoracic extension of retroperitoneal urine collections. *AJR Am J Roentgenol*. 1981;137(1):37-41. <https://doi.org/10.2214/ajr.137.1.37>
26. Adam WR, Arkles LB, Gill G, Meagher EJ, Thomas GW. Hydrothorax with peritoneal dialysis: radionuclide detection of a pleuro-peritoneal connection. *Aust N Z J Med*. 1980;10(3):330-2. <https://doi.org/10.1111/j.1445-5994.1980.tb04080.x>
27. Rocco M, Carbone I, Morelli A, Bertoletti L, Rossi S, Vitale M, et al. Diagnostic accuracy of bedside ultrasonography in the ICU: feasibility of detecting pulmonary effusion and lung contusion in patients on respiratory support after severe blunt thoracic trauma. *Acta Anaesthesiol Scand*. 2008;52(6):776-84. <https://doi.org/10.1111/j.1399-6576.2008.01647.x>
28. Grimberg A, Shigueoka DC, Atallah AN, Ajzen S, Iared W. Diagnostic accuracy of sonography for pleural effusion: systematic review. *Sao Paulo Med J*. 2010;128(2):90-5. <https://doi.org/10.1590/s1516-31802010000200009>
29. Röthlin MA, Näf R, Amgwerd M, Candinas D, Frick T, Trentz O. Ultrasound in blunt abdominal and thoracic trauma. *J Trauma*. 1993;34(4):488-95. <https://doi.org/10.1097/00005373-199304000-00003>
30. Wang AYM, Sanderson JE. Current perspectives on diagnosis of heart failure in long-term dialysis patients. *Am J Kidney Dis*. 2011;57(2):308-19. <https://doi.org/10.1053/j.ajkd.2010.07.019>
31. Gargani L. Lung ultrasound: a new tool for the cardiologist. *Cardiovasc Ultrasound*. 2011;9:6. <https://doi.org/10.1186/1476-7120-9-6>
32. Noble VE, Murray AF, Capp R, Sylvia-Reardon MH, Steele DJR, Liteplo A. Ultrasound assessment for extravascular lung water in patients undergoing hemodialysis. Time course for resolution. *Chest*. 2009;135(6):1433-9. <https://doi.org/10.1378/chest.08-1811>
33. Zoccali C, Torino C, Tripepi R, Tripepi G, D'Arrigo G, Postorino M, et al. Pulmonary congestion predicts cardiac events and mortality in ESRD. *J Am Soc Nephrol*. 2013;24(4):639-46. <https://doi.org/10.1681/ASN.2012100990>
34. Copetti R, Soldati G, Copetti P. Chest sonography: a useful tool to differentiate acute cardiogenic pulmonary edema from acute respiratory distress syndrome. *Cardiovasc Ultrasound*. 2008;6:16. <https://doi.org/10.1186/1476-7120-6-16>
35. Liteplo AS, Marill KA, Villen T, Miller RM, Murray AF, Croft PE, et al. Emergency thoracic ultrasound in the differentiation of the etiology of shortness of breath (ETUDES): sonographic B-lines and N-terminal pro-brain-type natriuretic peptide in diagnosing congestive heart failure. *Acad Emerg Med*. 2009;16(3):201-10. <https://doi.org/10.1111/j.1553-2712.2008.00347.x>
36. Gargani L, Soliman-Aboumarie H, Volpicelli G, Corradi F, Pastore MC, Cameli M. Why, when, and how to use lung ultrasound during the COVID-19 pandemic: enthusiasm and caution. *Eur Heart J Cardiovasc Imaging*. 2020;21(9):941-8. <https://doi.org/10.1093/ehjci/jeaa163>



## ERRATUM

<https://doi.org/10.1590/1806-9282.20210476ERRATUM>

In the manuscript “Lung ultrasound: an opportunity to increase the accuracy of the physical examination by the nephrologist”, DOI: 10.1590/1806-9282.20210476, published in the Rev Assoc Med Bras. 2021;67(11):1729-1734, on page 1731, figure 4:

### Where it reads:

**Figure 4.** Lung ultrasound from a patient with COVID-19 showing an irregular and fragmented pleural line from which a B-line originates.

### It should read:

**Figure 4.** Lung ultrasound from a patient with COVID-19 showing an irregular and fragmented pleural line from which a B-line originates. (Image courtesy of Professor José M. Pazeli Jr.)